

# Tunable topological electronic structure of silicene on a semiconducting Bi/Si(111)- $\sqrt{3}\times\sqrt{3}$ substrate

Zhi-Quan Huang,<sup>1</sup> Bo-Hung Chou,<sup>1</sup> Chia-Hsiu Hsu,<sup>1</sup> Feng-Chuan Chuang,<sup>1,\*</sup> Hsin Lin,<sup>2,†</sup> and Arun Bansil<sup>3</sup><sup>1</sup>*Department of Physics, National Sun Yat-Sen University, Kaohsiung 804, Taiwan*<sup>2</sup>*Graphene Research Centre and Department of Physics, National University of Singapore, Singapore 117542, Singapore*<sup>3</sup>*Department of Physics, Northeastern University, Boston, Massachusetts 02115, USA*

(Received 8 August 2014; revised manuscript received 15 December 2014; published 29 December 2014)

Using first-principles calculations to obtain the crystal and electronic structures, we show that the  $1\times 1$  phase of silicene is energetically more favorable than the  $\sqrt{3}\times\sqrt{3}$  silicene superstructure on a semiconducting Bi/Si(111)- $\sqrt{3}\times\sqrt{3}$  substrate. The band gap of the system is found to be influenced strongly through the participation of Bi orbitals, which possess a larger spin-orbit coupling strength compared to Si. In particular, the nontrivial (topological) band gap of a few meV in freestanding  $1\times 1$  silicene enlarges to 124 meV and becomes trivial in the presence of the substrate. We further show how an out-of-the-plane external electric field can be used to tune the band gap and restore the nontrivial topological phase.

DOI: [10.1103/PhysRevB.90.245433](https://doi.org/10.1103/PhysRevB.90.245433)

PACS number(s): 73.20.-r, 77.22.Ej, 77.55.-g

## I. INTRODUCTION

Silicene, a one-atom-thick two-dimensional (2D) crystal of silicon with a hexagonal lattice structure like graphene [1], has generated enormous interest since it was first proposed theoretically [2]. Freestanding silicene was predicted to be a 2D topological insulator (TI) or a quantum spin Hall (QSH) insulator [3–6]. The characteristic feature of TIs is that these novel materials are insulators in the bulk, but harbor gapless edge states on the boundaries protected by constraints of time-reversal symmetry. Numerous studies have shown that silicene could be grown on various metallic substrate such as Ag(111) [7–13], Ir(111) [14], and Au(110) [15]. Lattice mismatch between silicene and the metallic substrate results in many surface reconstructions, and the  $\sqrt{3}\times\sqrt{3}$  [11,12],  $2\sqrt{3}\times 2\sqrt{3}$  [7,8],  $\sqrt{7}\times\sqrt{7}$  [10], and  $3\times 3$  [10] phases have been reported experimentally. The disadvantage of growing silicene on a metallic substrate is that the band topology is ill-defined in a metallic system. Moreover, metallic substrates do not retain the  $1\times 1$  pristine phase of silicene. It is highly desirable therefore to explore other substrates, which can support a nearly freestanding silicene.

Metallic elements such as those of groups III (Al, Ga, In, Tl), IV (Pb and Sn), and V (As, Sb, Bi) have been studied extensively on the Si(111) substrate, where they act as a surfactant cover on the Si(111) surface, and yield a rich tapestry of phases with interesting electronic properties [16–21]. In particular, the structural model of Bi adsorbed on Si(111) has been investigated experimentally [22–27] as well as theoretically [25]. The well-known structural reconstruction proposed for the  $\sqrt{3}\times\sqrt{3}R30^\circ$  phase (hereafter referred to as the  $\sqrt{3}$  phase) consists of trimers (milkstool model) at 1 ML coverage [25,28]. The Bi/Si(111)- $\sqrt{3}$  discussed in this article is an example of a semiconducting substrate with metallic bonding via the Bi trimer layer lying on its top. The idea of growing silicene in this way is in the spirit of growing graphene on metal-intercalated substrates [29,30]. Notably, the lattice

of Si(111) substrate is essentially perfectly matched to that of silicene. Interestingly, the underlying Bi bilayers can enhance spin-orbit coupling effects and induce Rashba spin splitting of states in the surface [29,31,32].

In this study, we employ first-principles calculations to delineate the crystal and electronic structures of Bi-intercalated silicene/Si(111) at 1 ML Bi coverage. The lowest-energy atomic configuration of the buckled silicene layer is identified. The combined system exhibits charge transfer from silicene to the underlying layer of Bi trimers. By direct evaluation of the  $Z_2$  topological invariant as well as by using adiabatic continuity arguments, we show that the Bi-intercalated silicene/Si(111) system is a topologically trivial insulator. However, an out-of-the-plane external electric field turns the system into a  $Z_2$  topological insulator with a band gap larger than that of freestanding silicene.

## II. COMPUTATIONAL METHODS

The present calculations were carried out by employing the Perdew-Burke-Ernzerhof exchange functional [33] to the density-functional theory (DFT) [34] using the projector-augmented-wave (PAW) [35] scheme as implemented in the Vienna *ab initio* simulation package (VASP) [36]. A vacuum layer of 20 Å was included in the supercell to model the 2D system. For structural relaxation, three Si(111) bilayers were used as the substrate, where Si atoms in the bottom layer were passivated by H atoms. Except for the bottom Si bilayer and the associated H atoms, all other atoms were relaxed until the residual force on each atom was smaller than 0.001 eV/Å. The cutoff kinetic energy was set at 250 eV. A  $\Gamma$ -centered  $12\times 12\times 1$  Monkhorst-Pack [37] grid was used for structural relaxations. All electronic structure computations were converged to a self-consistency of  $10^{-6}$  eV. Spin-orbit coupling (SOC) was included in self-consistency cycles and band computations throughout this work unless specified otherwise.

## III. RESULTS AND DISCUSSION

The surface lattice constant of Si(111)- $\sqrt{3}\times\sqrt{3}$  is 6.70 Å. Stabilities of various structural models were considered by

\*fchuang@mail.nsysu.edu.tw

†nilnish@gmail.com

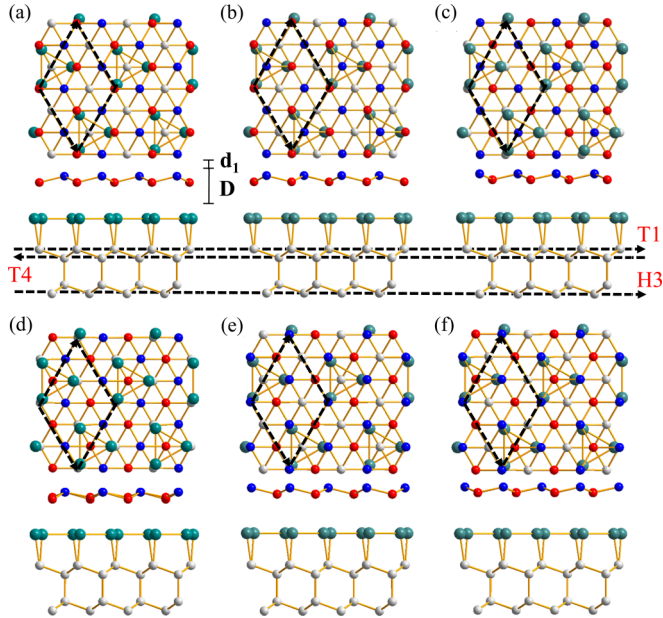


FIG. 1. (Color online) Various different models of Bi-intercalated silicene on Si(111)- $\sqrt{3}\times\sqrt{3}$ . White and dark green spheres denote Si and Bi atoms, respectively. The blue (red) spheres represent atoms in the top (bottom) layer of silicene. The relevant structural information is summarized in Table I.

defining the formation energy  $E_f$  as

$$E_f = E_{\text{tot}} - E_{\text{sub}} - E_{\text{silicene}}, \quad (1)$$

where  $E_{\text{tot}}$  is total energy of silicene on Bi/Si(111)- $\sqrt{3}$ ,  $E_{\text{sub}}$  is total energy of the Bi/Si(111)- $\sqrt{3}$  substrate, and  $E_{\text{silicene}}$  is the total energy of freestanding silicene. Here, we assume that freestanding silicene and Bi/Si(111)- $\sqrt{3}$  are both stable phases, and the formation energy is the energy difference resulting from the merging of the two systems. The phonon zero-point energy was not included in our computations. The negative value of formation energy implies that the merged system is more stable compared to the two separated systems.

The lowest-energy model for Bi on Si(111)- $\sqrt{3}$  at 1-ML coverage is the well-known trimer model in which the triangular center is located above the so-called H3 site and the three Bi atoms lie near the T1 site [25]. Accordingly, we examined different structural models for the growth of silicene on Bi/Si(111)- $\sqrt{3}$  where atoms of top and bottom layers of silicene can locate iteratively above the T1, or T4, or H3 sites, as shown in Figs. 1(a)–1(c), leading to a total of six structural models. Note that the atop T1 site lies above the topmost Si atom, the fourfold coordinated T4 site lies above the second layer Si atom, and the threefold hollow H3 site lies on top of the center of the honeycomb in the first bilayer. For example, the T4-T1 model has the upper layer of silicene at the T4 site, while the lower layer is at the T1 site. All investigated structures were fully relaxed. The relevant data for various structural models are summarized in Table I. Models with Si atoms of the lower layer in silicene lying at the T1 site are generally seen to be of lower energy from the results of Table I, with the T4-T1 model displaying the lowest energy among the six models considered.

TABLE I. Structural parameters for six different models of silicene considered in Fig. 1. Positions of the top and bottom Si atoms with respect to the Si(111) substrate and the corresponding formation energies,  $E_f$ , are given.  $d_1$  is the vertical distance between the buckled silicene layers, while  $D$  is the vertical distance between the bottom layer of silicene and the Bi atoms of the substrate, see Fig. 1.

Model Figure	Top-bottom Si (Site)	$E_f$ (eV)	$d_1$ (Å)	$D$ (Å)
1(a)	(T4-T1)	-0.1617	0.5620	3.2297
1(b)	(H3-T1)	-0.0733	0.5506	3.2599
1(c)	(H3-T4)	0.0150	0.5305	3.3372
1(d)	(T4-H3)	0.0160	0.5292	3.3131
1(e)	(T1-T4)	0.0176	0.5089	3.3792
1(f)	(T1-H3)	0.0931	0.5097	3.5652

The  $\sqrt{3}\times\sqrt{3}$  phase of silicene has been observed experimentally on Ag(111) [11,12], where the three Si atoms are raised and lowered alternatively to create the  $\sqrt{3}$  pattern. We have tested the viability of using these  $\sqrt{3}$  structures as the initial crystal structures on both Ag(111) and Bi/Si(111)- $\sqrt{3}$  substrates, and find that the minimum energy structures of silicene are substrate dependent. For silicene/Ag(111), the relaxed structure remains  $\sqrt{3}$ , in agreement with experimental observations [9]. For the Bi/Si(111)- $\sqrt{3}$  substrate, on the other hand,  $\sqrt{3}$  phase possesses a higher energy and the system relaxes back to  $1\times 1$  silicene. Notably, as a whole, in the minimum energy system of silicene on Bi/Si(111)- $\sqrt{3}$ , the supercell is  $\sqrt{3}\times\sqrt{3}$ , which is defined by the Bi patterns of the substrate, but the crystal structure of the silicene layer part is similar to that of freestanding silicene and not  $\sqrt{3}$ .

We focus now on analyzing the electronic structure of the lowest energy Bi-intercalated T4-T1 model of Fig. 1(a). In this connection, the surface Brillouin zones (SBZ) of the  $1\times 1$  and  $\sqrt{3}\times\sqrt{3}$  structures are outlined in Fig. 2(a) with red and black lines, respectively. Figure 2(b) shows the band structure for the T4-T1 model along the  $M' - \Gamma - K' - M'$  line, where the bands have been unfolded into the  $1\times 1$  SBZ. Red circles give the band structure of  $1\times 1$  silicene, with the sizes of circles being proportional to the weights of silicene contribution to various bands. The substrate is seen to enhance the band gap, which occurs at the  $K$  point, to 124 meV, compared to a value of only a few meV in freestanding silicene. However, the valence band of silicene now connects with that from Bi trimers, and the system becomes metallic, and it is no longer in the topological phase of freestanding silicene. In fact, the aforementioned 124-meV band gap is not driven by the SOC, and remains large (163 meV) even when the SOC is artificially turned off in the calculations.

The band gap in freestanding silicene can be controlled via an out-of-the-plane external electric field ( $E$  field) [6,38]. In Fig. 3(b), we have set the  $E$  field to point along the negative  $z$  axis because if the electric field is taken to point along the positive  $z$  axis, it will induce more charge to be transferred from silicene to Bi trimers, making the system more metallic, which is not desirable. The electric field of the surface dipole acts like an external field and the substrate thus breaks the inversion symmetry of silicene. In fact, silicene provides

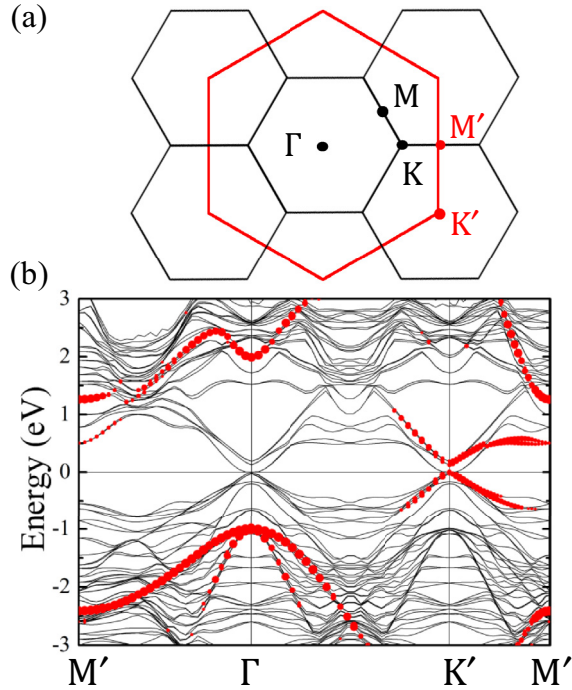


FIG. 2. (Color online) (a) Surface Brillouin zones for silicene  $1 \times 1$  (red lines) and silicene on  $\text{Bi/Si}(111)\text{-}\sqrt{3} \times \sqrt{3}$  (black lines). (b) Band structure for the T4-T1 model along the  $M' - \Gamma - K' - M'$  symmetry lines, where the bands have been unfolded into the  $1 \times 1$  SBZ. Red circles give the band structure of  $1 \times 1$  silicene, with the sizes of circles being proportional to the weights of silicene contribution to various bands.

electrons to Bi trimers in Fig. 2(b). We have verified this by observing a holelike Fermi surface (FS) from silicene and an electronlike FS from Bi in the band structure of the combined silicene-substrate system. The band structure when an  $E$  field of  $0.4 \text{ V/\AA}$  is present along the  $-z$  axis is shown in Fig. 3(a). The external field balances that due to surface dipoles, and there is little net charge transfer between silicene and Bi atoms. The system becomes insulating with a band gap of  $8 \text{ meV}$  at the  $\Gamma$  point. In this way, the external  $E$  field provides a mechanism for producing spin-polarized states and realizing a gating controlled topological phase transition. Figures 3(c)–3(e) show band structures around  $\Gamma$  for three different applied  $E$  fields. A topological phase transition is seen to take place around  $0.408 \text{ V/\AA}$  where the band gap closes at  $\Gamma$  [39].

In order to ascertain the topology of the band structure in the presence of an external electric field, we follow the method of Ref. [40] for computing the  $Z_2$  invariant in terms of the so-called  $n$ -field configuration of system, which is shown in Fig. 4 for applied field strengths of  $0.05$  and  $0.5 \text{ V/\AA}$ . Quantum spin hall (QSH) states are characterized by  $Z_2$  topological numbers. The method involves creating a uniform grid in the first Brillouin zone and counting the vorticities associated with the zeros of the pfaffian in half the Brillouin zone. The  $n$ -field configuration indicates the properties and distribution of vorticities. The white and black circles denote  $n = +1$  and  $-1$ , respectively, while the blanks denotes  $0$ . The  $Z_2$  invariant is then obtained by summing the  $n$ -field over half of the torus formed by the  $G_1$  and  $G_2$  reciprocal space vectors. For a field

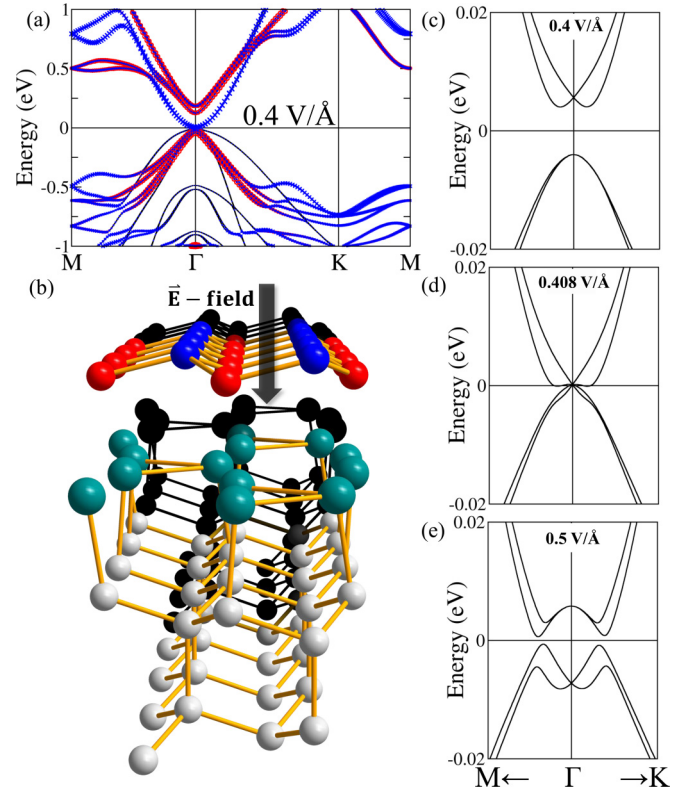


FIG. 3. (Color online) Band structure of the most stable (T4-T1) model under an out-of-the-plane  $E$  field of  $0.4 \text{ V/\AA}$ . Red circles (blue crosses) give the contribution of silicene (Bi) to various bands. (b) Schematic diagram of the T4-T1 model subjected to a transverse external electric field. (c)–(e) Blow ups of band structures around the  $\Gamma$  point for three different values of the electric field showing the critical point at  $0.408 \text{ V/\AA}$  in (d).

of  $0.5 \text{ V/\AA}$ , we thus obtain a nontrivial  $Z_2$  value of  $1$ , while for  $0.05 \text{ V/\AA}$ , the  $Z_2$  value is  $0$ , confirming that the system undergoes a topological phase transition between these two field values.

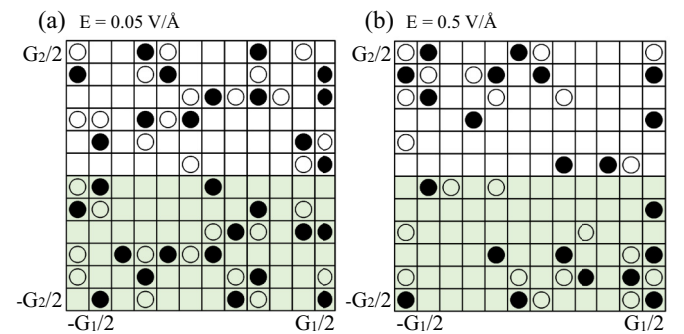


FIG. 4. (Color online) The  $n$ -field configuration for silicene on  $\text{Bi/Si}(111)\text{-}\sqrt{3}$  for an external electric field of (a)  $0.05$  and (b)  $0.5 \text{ V/\AA}$  over the torus in the Brillouin zone spanned by the reciprocal lattice vectors  $G_1$  and  $G_2$ . White and black circles denote  $n = +1$  and  $-1$ , respectively, while the blank denotes  $0$ . The  $Z_2$  invariant is obtained by summing the  $n$  field over half of the torus defined by vectors  $G_1$  and  $G_2$ .  $Z_2$  is  $0$  (trivial) in (a) and  $1$  (nontrivial) in (b).



We note that the closing and reopening of the band gap in silicene on Bi/Si(111)- $\sqrt{3}$  under an out-of-the-plane electric field takes place near the  $\Gamma$  point, which is different from the  $K$  point at which the band gap is located in freestanding silicene. An analysis of the orbital characters indicates that this effect is not merely a consequence of band folding reflecting the mapping of the  $K$  point of the  $1\times 1$  unit cell to the  $\Gamma$  point of the  $\sqrt{3}\times\sqrt{3}$  supercell. In freestanding silicene, bands near the Fermi level originate from  $p_z$  orbitals of Si atoms, and the size of the band gap is limited by the strength of SOC of Si. As shown in Fig. 3(a), for silicene on Bi/Si(111)- $\sqrt{3}$ , on the other hand, while the valence bands are primarily associated with Si, the conduction bands mainly arise from Bi. Therefore the band gap in the nontrivial phase under the electric field can be larger due to the stronger SOC of Bi compared to Si.

In order to examine the robustness of our results, we have considered the effect of extending the size of the vacuum layer to 38 Å, as well as that of relaxing the atomic structure in the presence of electric field. In these two test computations, we found the magnitude of field needed to recover the topological phase to be around 0.408 V/Å. We also considered effects of increasing the number of bilayers in the substrate to four, five and six. A topological phase transition was still observed, although the magnitude of  $E$  field needed to recover the topological phase is reduced to 0.22, 0.103, and 0.063 V/Å with increasing number of substrate layers. The slow convergence of the critical field here is due to poor screening in the semiconducting substrate. Assuming an exponential decay with layer thickness, we obtain an estimate of the critical field of 0.025 V/Å for an infinite number of substrate layers. Such an electric field could be realized in a gating device by using modern semiconductor fabrication techniques.

#### IV. CONCLUSION

To summarize, using first-principles calculations, we have investigated the crystal and electronic structures of silicene on a Bi/Si(111)-( $\sqrt{3}\times\sqrt{3}$ ) substrate. The  $1\times 1$  structure of freestanding silicene is found to be stable without the reconstructions of silicene commonly seen on various metallic substrates. Although the Bi-intercalated Si(111) substrate destroys the topological phase of pristine silicene, we show how this phase can be restored by applying an external out-of-the-plane electric field to drive the system through a topological phase transition. Our identification for the first time of a substrate that could support the  $1\times 1$  structure of pristine silicene, paves the way for exploiting novel properties of this material for fundamental science studies as well as applications.

#### ACKNOWLEDGMENTS

FCC acknowledges support from the National Center for Theoretical Sciences and Ministry of Science and Technology of Taiwan under Grant Nos. MOST-101-2112-M-110-002-MY3 and MOST-101-2218-E-110-003-MY3, and the support the National Center for High Performance Computing for computer time and facilities. The work at Northeastern University was supported by the US Department of Energy (DOE), Office of Science, Basic Energy Sciences grant number DE-FG02-07ER46352 (core research), and benefited from Northeastern University's Advanced Scientific Computation Center (ASCC), the NERSC supercomputing center through DOE grant number DE-AC02-05CH11231, and support (applications to layered materials) from the DOE EFRC: Center for the Computational Design of Functional Layered Materials (CCDM) under DE-SC0012575. H.L. acknowledges the Singapore National Research Foundation for support under NRF Award No. NRF-NRFF2013-03.

- 
- [1] K. S. Novoselov, A. K. Geim, S. V. Morozov, D. Jiang, Y. Zhang, S. V. Dubonos, I. V. Grigorieva, and A. A. Firsov, *Science* **306**, 666 (2004).
  - [2] G. G. Guzmán-Verri and L. C. Lew Yan Voon, *Phys. Rev. B* **76**, 075131 (2007).
  - [3] C.-C. Liu, W. Feng, and Y. Yao, *Phys. Rev. Lett.* **107**, 076802 (2011).
  - [4] L. Fu and C. L. Kane, *Phys. Rev. B* **76**, 045302 (2007).
  - [5] X.-L. Qi and S.-C. Zhang, American Institute of Physics, S-0031-9228-1001-020-3 (2009).
  - [6] W.-F. Tsai, C.-Y. Huang, T.-R. Chang, H. Lin, H.-T. Jeng, and A. Bansil, *Nat Commun.* **4**, 1500 (2013).
  - [7] A. Kara, H. Enriquez, Ari P. Seitsonen, L. C. Lew Yan Voon, S. Vizzini, B. Aufray, and H. Oughaddou, *Surf. Sci. Rep.* **67**, 1 (2012).
  - [8] B. Lalmi, H. Oughaddou, H. Enriquez, A. Kara, S. Vizzini, B. Ealet, and B. Aufray, *Appl. Phys. Lett.* **97**, 223109 (2010).
  - [9] P. Vogt, P. D. Padova, C. Quaresima, J. Avila, E. Frantzeskakis, M. C. Asensio, A. Resta, Bénédicte Ealet, and Guy Le Lay, *Phys. Rev. Lett.* **108**, 155501 (2012).
  - [10] B. Feng, Z. Ding, S. Meng, Y. Yao, X. He, P. Cheng, L. Chen, and K. Wu, *Nano Lett.* **12**, 3507 (2012).
  - [11] L. Chen, H. Li, B. Feng, Z. Ding, J. Qiu, P. Cheng, K. Wu, and S. Meng, *Phys. Rev. Lett.* **110**, 085504 (2013).
  - [12] P. D. Padova, P. Vogt, A. Resta, J. Avila, I. Razado-Colambo, C. Quaresima, C. Ottaviani, B. Olivieri, T. Bruhn, T. Hirahara, T. Shirai, S. Hasegawa, M. C. Asensio, and G. Le Lay, *Appl. Phys. Lett.* **102**, 163106 (2013).
  - [13] L. Chen, B. Feng, and K. Wu, *Appl. Phys. Lett.* **102**, 081602 (2013).
  - [14] L. Meng, Y. Wang, L. Zhang, S. Du, R. Wu, L. Li, Y. Zhang, G. Li, H. Zhou, W. A. Hofer, and H.-J. Ga, *Nano Lett.* **13**, 685 (2013).
  - [15] M. R. Tchalala, H. Enriquez, A. J. Mayne, A. Kara, S. Roth, M. G. Silly, A. Bendounan, F. Sirotti, T. Greber, B. Aufray, G. Dujardin, M. Ait Ali, and H. Oughaddou, *Appl. Phys. Lett.* **102**, 083107 (2013).
  - [16] J. M. Nicholls, B. Reihl, and J. E. Northrup, *Phys. Rev. B* **35**, 4137 (1987).
  - [17] A. Kawazu and H. Sakama, *Phys. Rev. B* **37**, 2704 (1988).
  - [18] H. B. Elswijk, D. Dijkkamp, and E. J. van Loenen, *Phys. Rev. B* **44**, 3802 (1991).
  - [19] M. Gothelid, M. Bjorkqvist, T. M. Grehk, G. Le Lay, and U. O. Karlsson, *Phys. Rev. B* **52**, R14352 (1995).

- [20] V. Yeh, L. Berbil-Bautista, C. Z. Wang, K. M. Ho, and M. C. Tringides, *Phys. Rev. Lett.* **85**, 5158 (2000).
- [21] M. H. Upton, C. M. Wei, M. Y. Chou, T. Miller, and T.-C. Chiang, *Phys. Rev. Lett.* **93**, 026802 (2004).
- [22] R. Shioda, A. Kawazu, A. A. Baski, C. F. Quate, and J. Nogami, *Phys. Rev. B* **48**, 4895 (1993).
- [23] R. Z. Bakhtizin, Ch. Park, T. Hashizume, and T. Sakurai, *J. Vac. Sci. Technol. B* **12**, 2052 (1994).
- [24] T. M. Schmidt, R. H. Miwa, and G. P. Srivastava, *Braz. J. Phys.* **34**, 629 (2004).
- [25] C. Cheng and K. Kunc, *Phys. Rev. B* **56**, 10283 (1997).
- [26] I. Gierz, T. Suzuki, E. Frantzeskakis, S. Pons, S. Ostanin, A. Ernst, J. Henk, M. Grioni, K. Kern, and C. R. Ast, *Phys. Rev. Lett.* **103**, 046803 (2009).
- [27] E. Frantzeskakis, S. Pons, and M. Grioni, *Phys. Rev. B* **82**, 085440 (2010).
- [28] C.-H. Hsu, H.-R. Chang, F.-C. Chuang, Y.-T. Liu, Z.-Q. Huang, H. Lin, V. Ozoliņš, and A. Bansil, *Surf. Sci.* **626**, 68 (2014).
- [29] C.-H. Hsu, V. Ozoliņš, and F.-C. Chuang, *Surf. Sci.* **616**, 149 (2013).
- [30] C.-H. Hsu, W.-H. Lin, V. Ozoliņš, and F. C. Chuang, *Appl. Phys. Lett.* **100**, 063115 (2012).
- [31] K. He, T. Hirahara, T. Okuda, S. Hasegawa, A. Kakizaki, and I. Matsuda, *Phys. Rev. Lett.* **101**, 107604 (2008).
- [32] E. Frantzeskakis, S. Pons, H. Mirhosseini, J. Henk, C. R. Ast, and M. Grioni, *Phys. Rev. Lett.* **101**, 196805 (2008).
- [33] J. P. Perdew, K. Burke, and M. Ernzerhof, *Phys. Rev. Lett.* **77**, 3865 (1996).
- [34] P. Hohenberg and W. Kohn, *Phys. Rev.* **136**, B864 (1964); W. Kohn and L. J. Sham, *ibid.* **140**, A1133 (1965).
- [35] P. E. Blochl, *Phys. Rev. B* **50**, 17953 (1994); G. Kresse and D. Joubert, *ibid.* **59**, 1758 (1999).
- [36] G. Kresse and J. Hafner, *Phys. Rev. B* **47**, 558 (1993); G. Kresse and J. Furthmuller, *ibid.* **54**, 11169 (1996).
- [37] H. J. Monkhorst and J. D. Pack, *Phys. Rev. B* **13**, 5188 (1976).
- [38] N. D. Drummond, V. Zolyomi, and V. I. Falko, *Phys. Rev. B* **85**, 075423 (2012).
- [39] We have tested the robustness of our results using PAW-LDA and PAW-GGA functionals, and found the gap size and the critical electric field to remain essentially changed. However, the phenomenon of recovering the nontrivial phase is intact.
- [40] T. Fukui and Y. Hatsugai, *J. Phys. Soc. Jpn.* **76**, 053702 (2007).